13

Measurement of Ultrashort Optical Pulses

Yuqiang Deng[1,*], Qing Sun[1], Shiying Cao[2],
Jing Yu[1], Ching-yue Wang[3] and Zhigang Zhang[4]
[1]*Optics Division, National Institute of Metrology, Beijing,*
[2]*Time and Frequency Center, National Institute of Metrology, Beijing,*
[3]*School of Precision Instrument and Optoelectronics Engineering,*
Tianjin University, Tianjin,
[4]*School of Electronics Engineering and Computer Science, Peking University, Beijing,*
P. R. China

1. Introduction

An ultrashort optical pulse has an extremely short duration period, an extremely broad spectral bandwidth, and an extremely high peak power [1]; it has therefore been widely used in a variety of applications, such as ultrafast pumping and detection, time-resolved spectroscopy, optical telecommunications, ultra-fine microfabrication, nonlinear optics and femtosecond chemistry. Femtosecond optical pulses have also brought revolutions in contemporary metrology [2], including time and frequency standards [3], terahertz metrology [4], and ultrafast electric pulses characterization [5]. Time domain waveform and pulse width are key parameters of the ultrashort optical pulses, because they directly affect experimental results acquired by use of ultrashort optical pulses. Experimental data cannot be deemed credible unless the waveform and pulse width are determined. Accurate knowledge of the temporal shape of optical pulses is therefore crucial to scientific research.

In the past three decades, several measurement techniques for ultrashort optical pulse have been developed. Autocorrelation (AC) [6], frequency-resolved optical gating (FROG) [7] and spectral phase interferometry for direct electric-field reconstruction (SPIDER) [8] are most commonly used. Autocorrelation is simple and convenient, but can give only the autocorrelation width; the waveform and phase is difficult to obtain. FROG is a two-dimensional measurement technique, pulse waveform and phase can be retrieved from the FROG trace, but an iterative procedure is needed. SPIDER can directly extract spectral phase and reconstruct pulse waveform; it is therefore suitable for accurate and fast measurement of ultrashort optical pulses, especially for the optical pulses in femtosecond range. In this chapter, we would introduce our technique for spectral phase retrieval to improve the accuracy of femtosecond optical pulses measurement, and demonstrate a versatile autocorrelator for ultrashort optical measurement, with which the time domain measurement range is greatly broaden.

* Corresponding Author

2. Characterization of femtosecond pulses with wavelet-transform for spectral phase retrieval

The spectrum of a pulse can easily be measured with a spectrometer. The pulse would be completely known, if we could, in addition, determine the phase across the spectrum [9]. SPIDER is a technique for measurement spectral phase of femtosecond optical pulses. In SPIDER setup, two replicas of the input pulse to be characterized are generated with a fixed time delay between them. These two replica pulses are then upconverted by sum-frequency mixing with a strongly chirped pulse derived from the same original input pulse. Because the two replica pulses are separated in time domain, they interact with different parts of the chirped pulse and are therefore upconverted to different frequencies. From the interferogram of these spectral shearing pulses, it is possible to extract the amplitude and phase of the initial pulse by using an algebraic inversion algorithm [2].

2.1 Optical schematics of SPIDER

Our home made SPIDER setup is shown in Fig. 1. Figure 1(a) is the schematic optical path. An input femtosecond laser pulse passes through an aperture A1, and then is reflected by a reflective mirror M1. The reflected pulse is split into two pulses by a beam splitter BS1. One of the split pulse is stretched into a strongly chirped pulse, and anther is fed into a Michelson-type interferometer and then replicate into two replicas. The Michelson-type interferometer consists of two beam splitters BS2, BS3 and two corner mirrors TS2, TS3. A fixed time delay between the replicas is generated by tuning the translation stage TS2. The strongly chirped pulse and the replicas are focused by a paraboloid mirror PM, and then sum-frequency generation occurs in a sum-frequency crystal CR. A translation stage TS1 is used for tuning the relative time delay between the strongly chirped pulse and the two replicas. The two replica pulses interact with different parts of the chirped pulse and are upconverted to two different frequencies. The spectral interferogram of the frequency upconverted pulses is recorded by a fiber spectrometer (HR 4000, Ocean Optics Inc.). The spectral phase of the input pulse can be retrieved from the measured spectral interferogram. Our home-made experimental optical setup is shown in Fig. 1(b), with the optical path superposed.

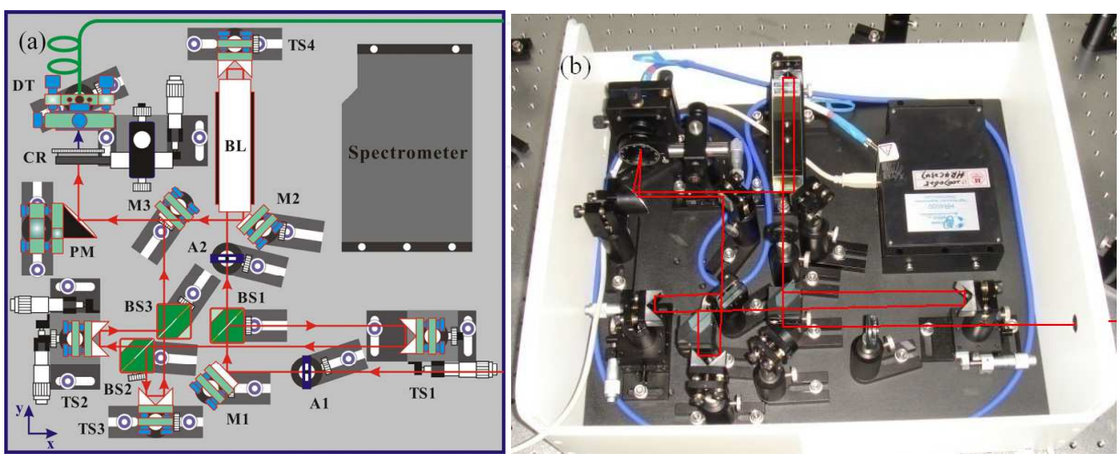

Fig. 1. Our home-made SPIDER setup and the optical path. (a) Optical schematic, (b) experimental setup.

2.2 Spectral phase retrieval with a wavelet-transfrom

In the traditional phase retrieval algorithm, spectral phase is extracted from the filtered alternating current component of the Fourier transform [8]. The filter is set by manual selection and adjustment. A problem is that different widths or shapes of the filter produce different spectral phases [10]. Thus the uncertainty of the spectral phase contributes to the uncertainty of the reconstructed pulses.

To reduce the uncertainty component coming from the filter with Fourier transform technique, we introduce a wavelet-transform for spectral phase retrieval of femtosecond optical pulses [11]. The phase is directly extracted from the ridge of wavelet-transform. There are no filters in this procedure so that the uncertainty from the filter is eliminated. In what fallows a demonstration of this procedure will be shown.

We have measured an ultrashort optical pulse train emitted from a Ti:sapphire laser (Micra-5, Coherent Inc.). The average output power of the laser is 360 mW after a pulse compressor. The repeat frequency is 82 MHz, and the central wavelength is 800 nm with a spectral bandwidth (FWHM) of 100 nm. We perform a SPIDER measurement with our home-made SPIDER setup. The measured spectral interferogram is shown in Fig. 2.

Wavelet-transform was applied on the measured spectral interferogram, and the time and frequency distributions are exhibited on a two-dimensional plane. The intensity map and phase map are shown in Figs. 3(a) and 3(b), respectively.

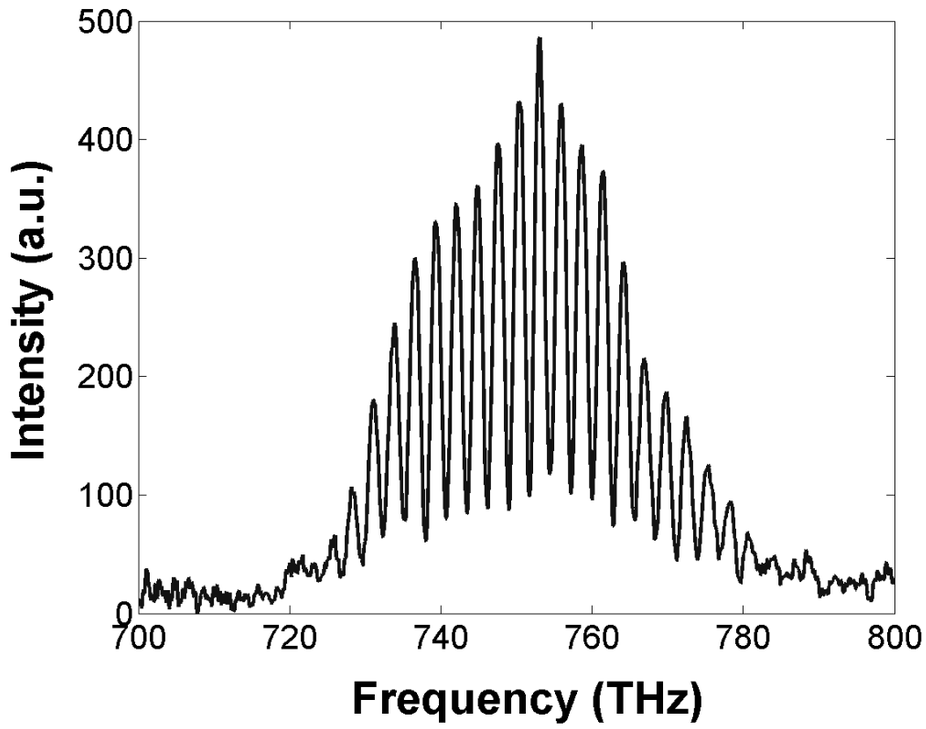

Fig. 2. Measured spectral interferogram.

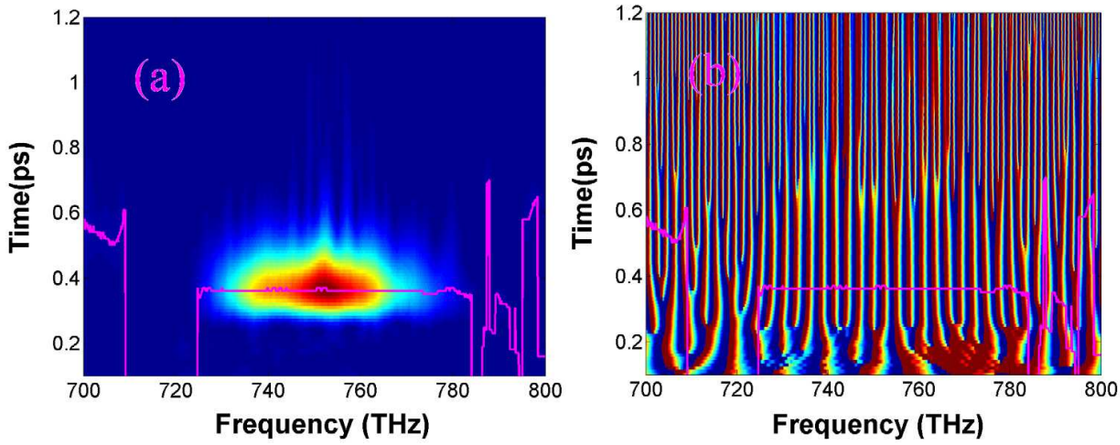

Fig. 3. Wavelet-transform of spectral interferogram. (a) Intensity topography, (b) phase topography. The ridge of wavelet-transform is indicated with a pink coloured line.

We search for the maximum values from the intensity topography along each frequency column. Connecting the positions of the maximum values at each frequency point constructs the ridge line of the wavelet-transform, which is superposed on Fig. 3(a) with a pink coloured line. Then we project the position of ridge from intensity topography (Fig. 3(a)) on the phase topography, as is shown in Fig. 3(b).

The phase of the spectral interferogram was directly extracted from the phase topography at the position of the ridge. With the extracted interferometry phase, the spectral phase was obtained with a concatenation algorithm [8], as is shown in Fig. 4.

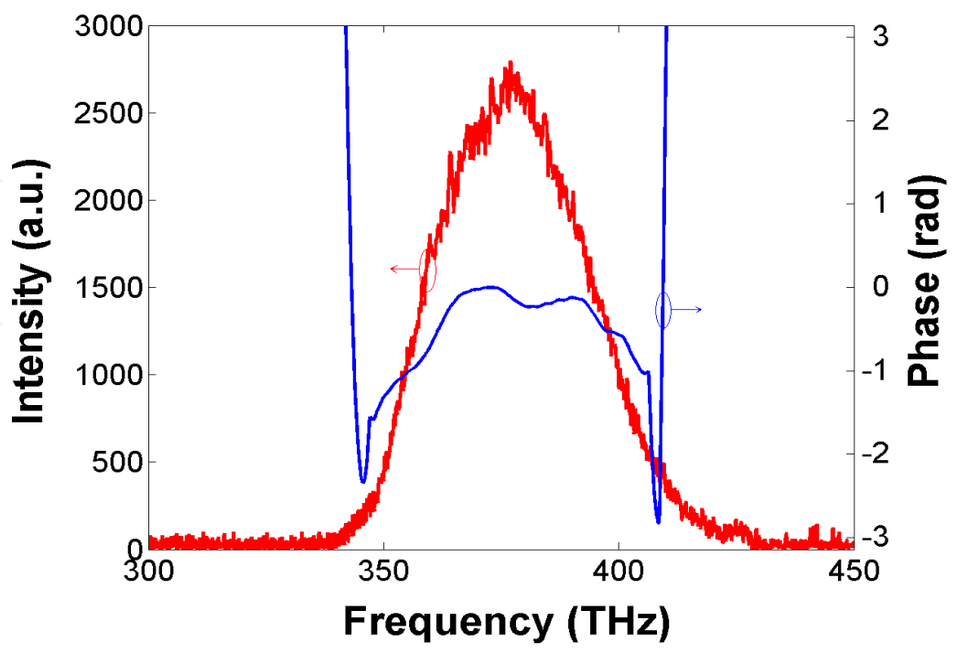

Fig. 4. Measured spectrum and retrieved spectral phase.

2.3 Pulse waveform reconstruction and autocorrelation simulation

Figure 4 shows the measured spectrum with a spectrometer (HR4000 CG-UV-NIR, Ocean Optics Inc.) and the retrieved spectral phase with wavelet-transform technique. The electric field (Fig. 5(a)) and waveform (Fig. 5(b)) of the femtosecond optical pulse are reconstructed from the spectrum and spectral phase with an inverse Fourier transform technique. The pulse width (FWHM) shown in Fig. 5(b) is 18.2 fs.

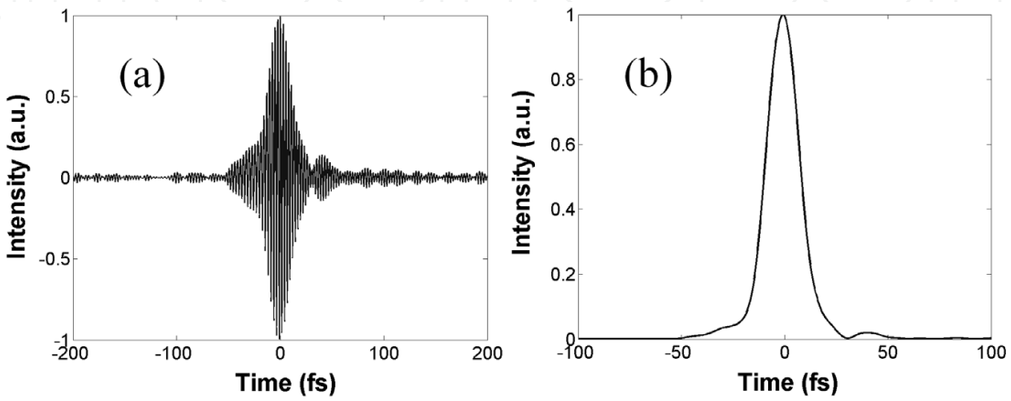

Fig. 5. Reconstructed electric field and waveform. (a) Electric field, (b) waveform.

From the reconstructed electric field in Fig. 5(a), we simulated the autocorrelation traces of the pulses. The simulated interferometric autocorrelation and intensity autocorrelation are shown in Fig. 6(a) and 6(b), respectively. The intensity autocorrelation in Fig. 6(b) shows the width of autocorrelation (FWHM) is 26.6 fs. With the reconstructed pulse waveform in Fig. 5(b) and the simulated intensity autocorrelation in Fig. 6(b), we can obtain the ratio of autocorrelation width τ_c to the pulse width τ_p is: $\tau_c/\tau_p = 1.462$.

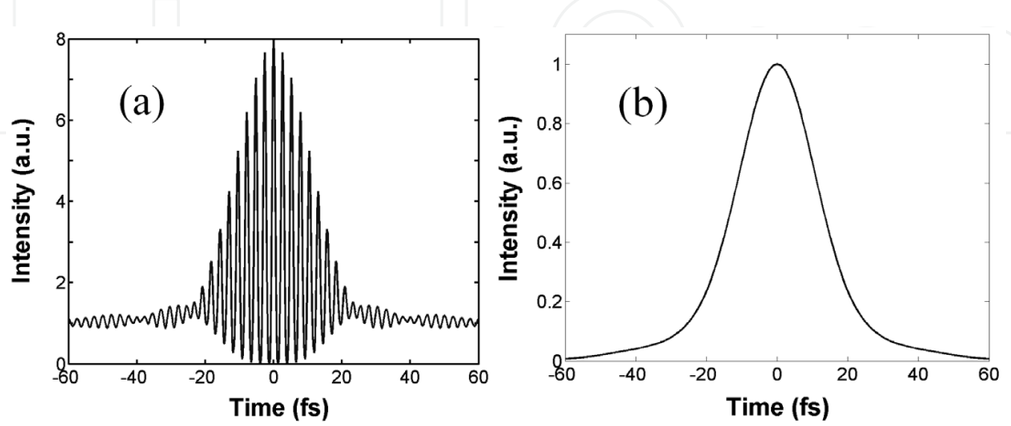

Fig. 6. Simulated autocorrelation traces with reconstructed pulse electric field.
(a) Interferomatric autocorrelation, (b) intensity autocorrelation.

2.4 Pulse waveform reconstruction from different replicas separations

We have investigated the effects of pulse replicas separation on the spectral phase retrieval of femtosecond optical pulses. By tuning the translation stage TS2, a serious of spectral interferograms with different replicas separations was recorded. Figures 7(a), 7(c), 7(e), 7(g), and 7(i) are five measured spectral interferograms with replicas separations of 0.22 ps, 0.55 ps, 0.83 ps, 1.58 ps, and 1.82 ps respectively. We retrieved the spectral phases from the five measured interferograms with wavelet-transfrom. The extracted spectral phases are shown in Figs. 7(b), 7(d), 7(f), 7(h), and 7(j).

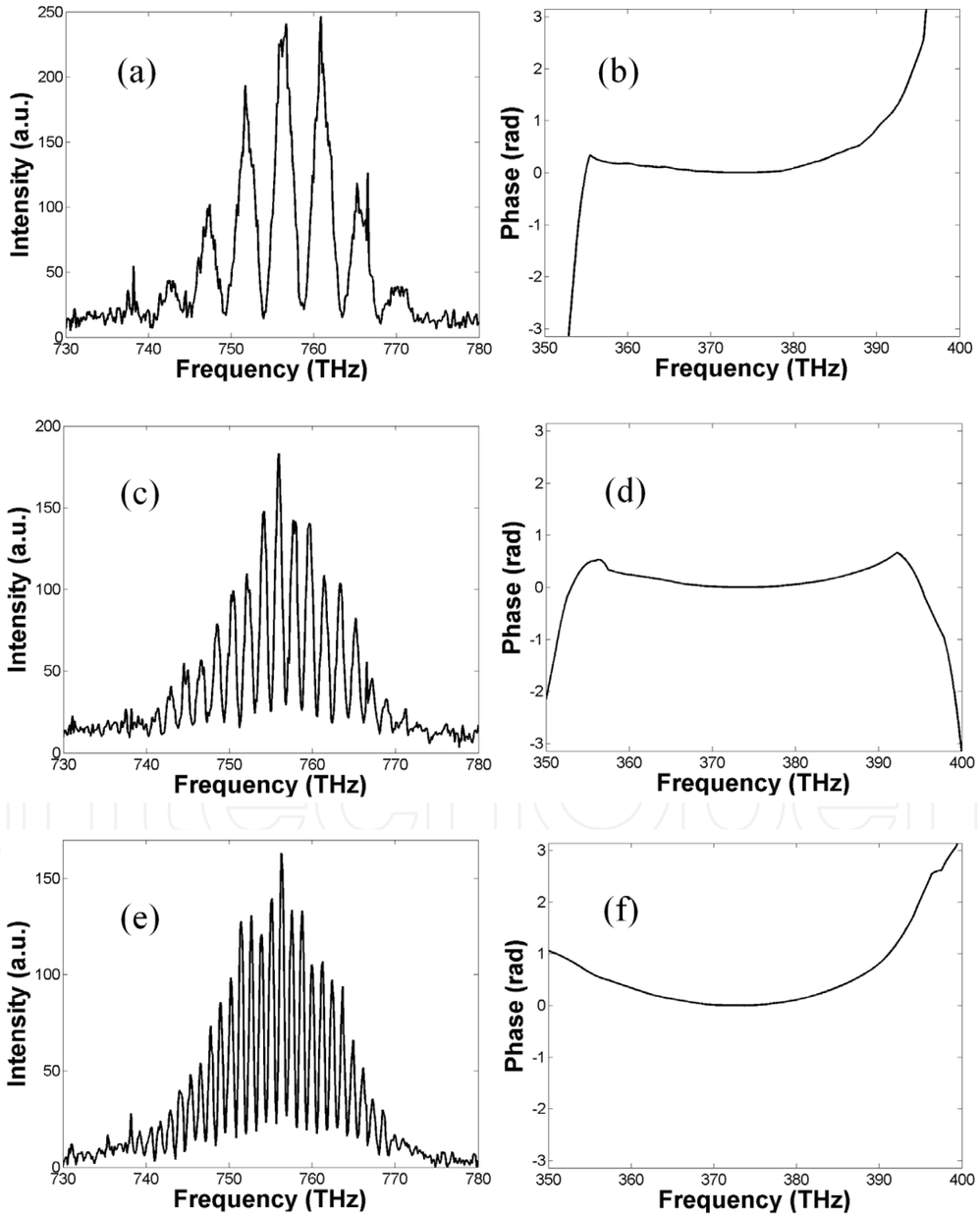

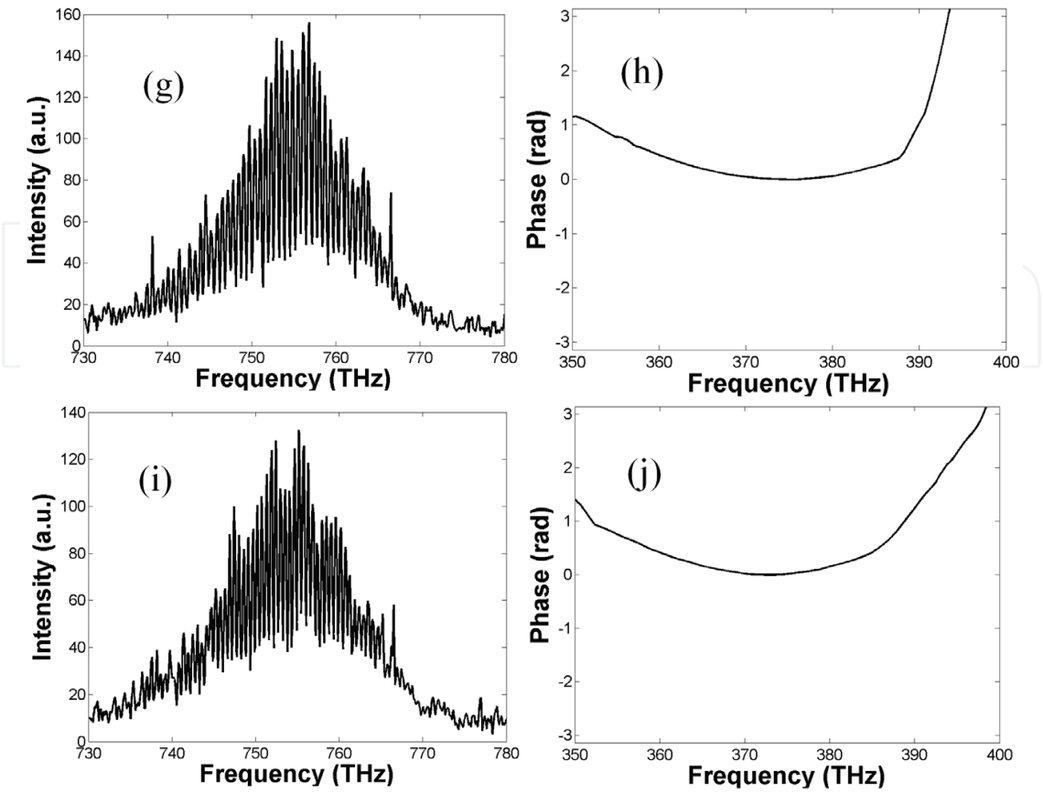

Fig. 7. Measured spectral interferograms with different replicas separations and retrived spectral phases from the interferograms. (a), (c), (e), (g), and (i) are measured interferograms with replicas separations of 0.22 ps, 0.55 ps, 0.83 ps, 1.58 ps, and 1.82 ps respectively; (b), (d), (f), (h), and (j) are the retrieved spectral phases from interfrograms in (a), (c), (e), (g), and (i) respectively.

With the retrieved spectral phases and the measured spectrum, the waveform of the pulse can be reconstructed. Figure 8(a) is the five retrieved spectral phases with different replicas separations and the spectrum. Figure 8(b) is the reconstructed pulse profiles from the spectrum and spectral phases with inverse Fourier transform.

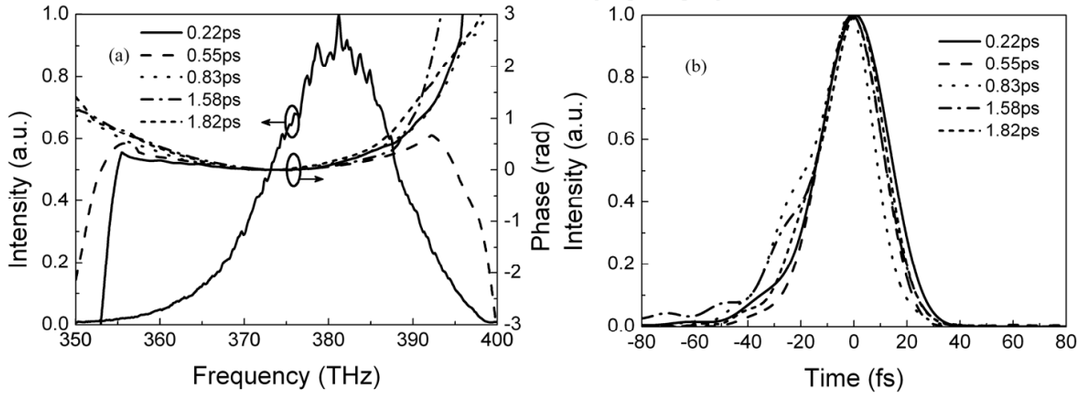

Fig. 8. Retrieved spectral phase and reconstructed pulse profile with different replicas separations. (a) Spectrum and retrieved spectral phases, (b) reconstructed pulse profiles.

Figure 8(a) shows that with wavelet transform, spectral phases are retrieved from a large range of replicas separations. With replicas separations from 0.22 ps to 1.82 ps, the relative difference of spectral phase is within 0.5 rad. In Fig. 8(b), the full width at half maximum (FWHM) of the reconstructed pulse profiles from replicas separations of 0.22 ps, 0.55 ps, 0.83 ps, 1.58 ps, and 1.82 ps are 28.50 fs, 27.30 fs, 27.77 fs, 28.75 fs, 28.47 fs, 26.81 fs, 26.65 fs, 27.60 fs, and 28.03 fs, respectively. The maximum relative difference is 2.76%, which demonstrates the accuracy of the spectral phase retrieval with wavelet-transform.

2.5 Uncertainty discussions

In the theory of inverse Fourier transform, reconstruction of pulse profile needs two parameters: spectrum and spectral phase. Broad spectrum of femtosecond optical pulse is measured with a spectrometer, which can be accurately calibrated by a black body or a standard lamp. Therefore, the uncertainty of spectral phase contribute majority of the uncertainty of pulse reconstruction. Uncertainty budget of spectral phase measurement is complex. We assume the laser source runs in a stable status, and the fluctuation of a mode-locked pulse is ignorable. The effects of the temperature and humidity of the surroundings on the chromatic dispersion of the measurement instrument is also ignorable. Therein we simply discuss the three main components for the uncertainty generation: measurement instrument (SPIDER setup), measured spectral interferogram, and algorithm of phase retrieval.

The chromatic dispersion of the beam splitter and the nonlinear crystal of the SPIDER setup generates an additional phase of the measured pulse. This additional phase shows an unnegligible effects in measurement of short pulses, especially in the case of pulse width less than 5 fs. Therefore, the thichness of beam splitters and the nonlinear crystals must be very small. To reduce the spectral phase retrieval error, the optical paths need carefully alignment for a high signal to noise ratio (SNR) interferogram recording. The spectral phase retrieval from interferograms with different replicas separations have been analyzed in section 2.4. The analysis and comparison of spectral phase retrieval error with wavelet-transform and Fourier transform with different filter widths is simulated and calculated in reference [10].

2.6 Comparison of wavelet-transform with Fourier transform

The comparison of spectral phase retrieval procedure with wavelet-transform and that with Fourier transform is plotted in Fig. 9. Figure 9(a) is the flow chart of phase retrieval by Fourier transform, and Fig. 9(b) is that by wavelet-transform.

From Fig. 9, we can see that phase retrieval procedure with wavelet-transform is much simpler. The phase reconstruction by Fourier transform includes three steps: Fourier transform, filtering, and inversed Fourier transform. In contrast, phase information can be read directly after the wavelet-transform, which saves two steps in the phase reconstruction, thus simplified the procedure. This simplified process eliminated the uncertainty coming from the filter with traditional Fourier transform; therefore more accurate spectral phase is retrieved. Another advantage of this simplified procedure is that the manual process of selection and adjustment filter is eliminated; therefore, the spectral phase compensation and control can realize automatic operation.

In principle, Fourier transform mixes all the time information of the spectral interferogram at different frequency position no mater whether there are signal or not, therefore, it is more prone to bring noise into signal information and result in pseudo phase.

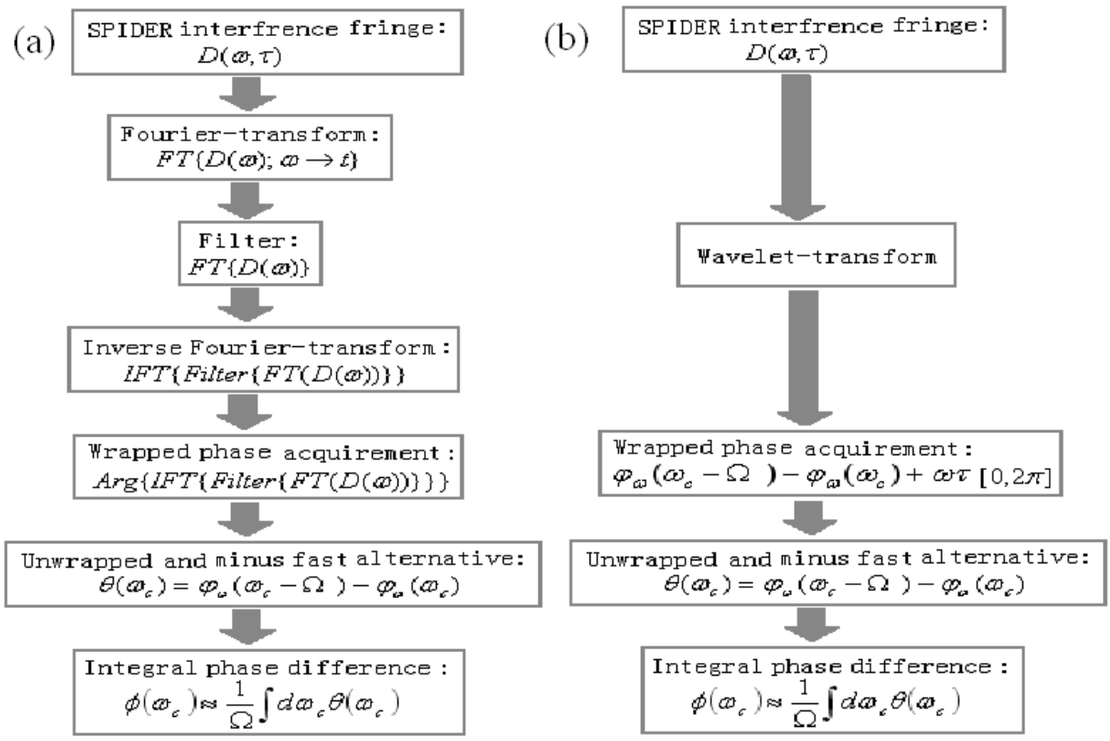

Fig. 9. Comparison of spectral phase retrieval flows between by Fourier transform and by wavelet-transform. (a) Flow chart of phase retrieval by Fourier transform, (b) by wavelet-transform.

However, the major advantage of phase reconstruction using wavelet-transform technique is that the wavelet-transform transfers the spectral interferogram into a two-dimensional graph that separates the signal from noise naturally. It does not need a filter to obtain phase information, but just probe the phase at the maximum of the transform. Therefore the error coming from the filter and the envelope noise is avoided; because there is no filter that needs to be judged by human, all the calculation can be processed automatically and is more suitable for video speed display.

3. Characterization of ultrashort optical pulses with autocorrelations

There are mainly two kinds of autocorrelations, i.e., intensity autocorrelations and interferometric autocorrelations [6]. Both of them have a Michelson-type interferometer setup. Intensity autocorrelation uses a translation stage scanning the split pulses to give an intensity envelope of the autocorrelation. The pulse width can be deduced from the width of the autocorrelation envelope. Intensity autocorrelation has a broad measurement range by use of the translation stage; however, it cannot provide complete information about the pulse shape. Interferometric autocorrelation uses a vibratile arm real-time scanning the split

pulses to generate a distinctive autocorrelation trace. The chirp and phase of the ultrashort optical pulse are reflected in the interferometric trace; however, the vibration range is limited in several hundred micrometers, which results in a limitation of measurement range with this technique. Therefore, a multifunctional autocorrelator, which can realize both interferometric autocorrelation and intensity autocorrelation, is desirable.

Meshulach *et al* have demonstrated a third-harmonic generation (THG) autocorrelator for ultrashort optical pulses measurement [12]. They used an ordinary glass slide as the THG source, and a pair of 32:1 THG interferometric autocorrelation trace and intensity autocorrelation trace were obtained. However, THG needs the input pulse have enough high energy, and the generated signal always has a low SNR in week energy conditions. In this letter, we demonstrate a second-harmonic generation (SHG) autocorrelator. We use a two-photon detector as the source of SHG. The setup is simplified, and the sensitivity is improved.

3.1 Optics schematics of a multifunctional autocorrelator

A multifunctional autocorrelator can be realized by use of a precise translation stage and a lock-in amplifier. The optical schematic is shown in Fig. 10(a). BS1 and BS2 are two 30/70 beam splitters coated with 450 nm - 1150 nm board bandwidth film, and M1 and M2 are two sliver roof mirrors. M2 was mounted on a translation stage (M405-DG, Physik Instrument GmbH), the resolution of which can reach 8.5 nm to provide a fine enough optical delay. We place a chopper (SR540, Stanford Research Systems Inc.) in the inlet of the incident pulse, and the output of a two-photon detector (G1115, Hamamatsu Photonics Corp.) is fed into a lock-in amplifier (SR830, Stanford Research Systems Inc.) to improve the SNR. Our home-made experimental setup of the multifunctional autocorrelator is shown in Fig. 10(b).

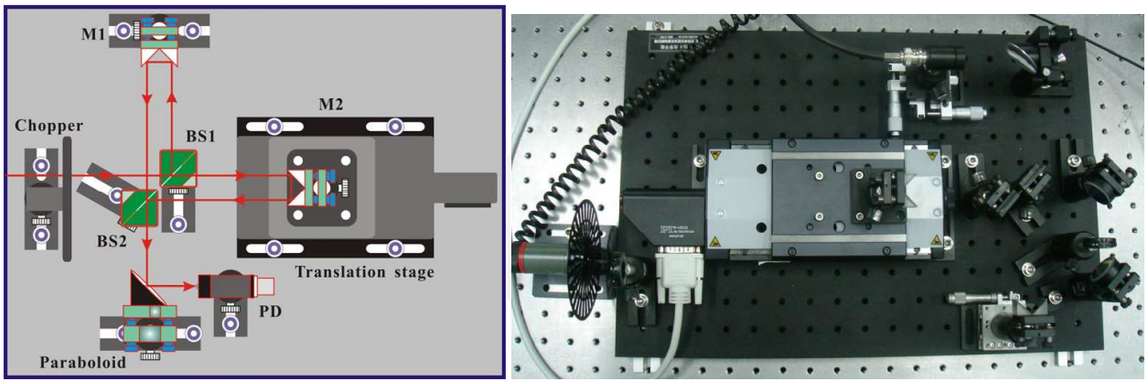

Fig. 10. Schematic of the versatile autocorrelator. M1, M2: Roof mirror; BS1, BS2: Beam splitter. (a) Optical schematic, (b) experimental setup.

The interferometric autocorrelation and intensity autocorrelation can be easily switched by tuning the scanning speed of the translation stage and the time constant of the lock-in amplifier. When the ratio of the central wavelength of the measured pulse λ_c to the time constant of the lock-in amplifier t_c is much less than two times of the scanning speed of the translation stage v_s, i.e., $\lambda_c / t_c << 2 \cdot v_s$, the measurement result shows an intensity

autocorrelation trace; When the ratio of the central wavelength λ_c to the time constant of the lock-in amplifier t_c is greatly larger than two times of the scanning speed of the translation stage v_s, i.e., $\lambda_c / t_c >> 2 \cdot v_s$, the measurement performs as an interferometric autocorrelation trace.

In section 2.2, we have measured the spectral interferogram of an ultrashort optical pulse train emitted from a Ti:sapphire laser (Micra-5, Coherent Inc.). In this section, we measure the autocorrelations of the same laser pulse with our home-made autocorrelator. By tuning the scanning speed of the translation stage and the time constant of the lock-in amplifier, both interferometric autocorrelation and intensity autocorrelation have been obtained. Figure 11(a) shows the intensity autocorrelation, and Fig. 11(b) shows the interferometric autocorrelation.

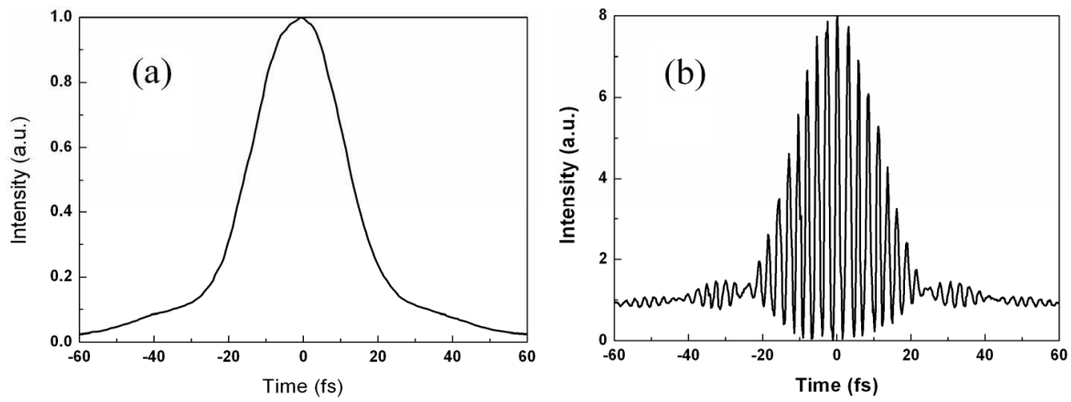

Fig. 11. Measured autocorrelation of Ti:sapphire laser pulses. (a) Interferometric autocorrelation, (b) intensity autocorrelation.

The intensity autocorrelation in Fig. 11(a) shows an autocorrelation width (FWHM) of 30 fs, and the corresponding pulses width is nearly 20 fs. And the interferometric autocorrelation in Fig. 11(b) shows the autocorrelation width and the chirp information. The interferometric autocorrelation has such a high SNR that the two wings of the interferometric trace can be clearly distinguished, which is useful in complete characterization of the ultrashort optical pulses.

From Fig. 11, we can see that the simulated autocorrelations are in good agreement with the simulated ones (in Fig. 6(b) and 6(a)). The deviation is within ±1 fs, which gives a proof of the reliability for both the techniques.

3.2 Measurement of a strongly chirped pulse

This autocorrelation setup is suitable for characterization of various ultrashort optical pulses, including strongly chirped pulses and fiber laser pulses. We use a 25-mm-thick SF 10 glass bulk to stretch the ultrashort optical pulses emitted from the Ti:sapphire laser. The chromatic dispersion of SF 10 glass is 156 fs^2 calculated with Sellmeier coefficient. And the width of critical pulse can be gotten with the equation:

$$T_c = 2\sqrt{\ln 2 \times \left|\ddot{\phi}\right|} = 104 \text{ fs}.$$

For a 15 fs nearly transform-limited ultrashort optical pulse, the output pulse width from the SF 10 glass is:

$$t_{p,out} = [1 + (T_c / t_p)^4]^{1/2} \cdot t_p = 720 \text{ fs}.$$

The pulses were stretched in temporal range with a great quadratic chirp, which can also be well characterized with the autocorrelator. The intensity autocorrelation and the interferometric autocorrelation were shown in Fig. 12(a) and 12(b), respectively.

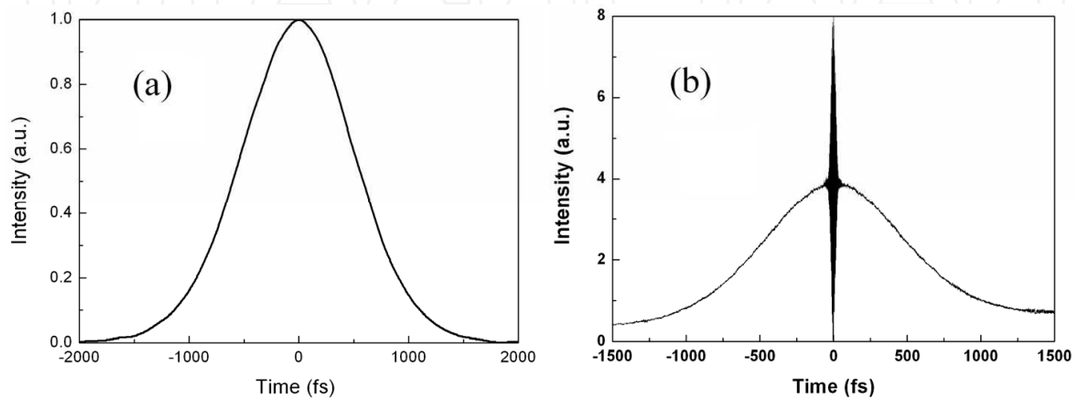

Fig. 12. Measured autocorrelation of the Ti:sapphire laser pulses stretched by a SF 10 glass bulk. (a) Interferometric autocorrelation, (b) intensity autocorrelation.

In Fig. 12(a), the intensity autocorrelation clearly shows the width of the broadened pulses. We can clearly discern the pulses width and the chirp of the pulses with the two autocorrelation traces, even if they have a great chirp. The intensity autocorrelation in Fig. 12(a) shows an autocorrelation width (FWHM) of 1100 fs, and the corresponding pulses width is 720 fs assuming a $Sech^2$-shaped pulses, which can agree well with the calculation of the stretched pulse. From Fig. 12(b), we can see that the interferometric autocorrelation shows the interference range is very narrow, and the two wings uplift, which demonstrated the great quadratic chirp generated from the dispersion of the SF 10 glass.

With the intensity autocorrelation and interferometric autocorrelation, both pulse width and phase information of the pulses were presented. Another advantage of this technique is that the space of the interferometric fringes can be used as a ruler to calibrate the time axis of the intensity autocorrelation. That is to say, this autocorrelator setup can self-calibrate with the two autocorrelation traces. This autocorrelation setup can give an accurate autocorrelation width of the pulses; however, a ratio factor should be assumed from autocorrelation width to pulse width. The ratio factor of different pulse waveforms varies greatly; therefore, unsuitable factor may generate great error in pulse width determination with autocorrelation.

3.3 Measurement of a fiber laser pulse

The autocorrelator also performs excellently in characterization of fiber lasers pulses. We measured a photonic crystal fiber laser (Ultrafast Laser Laboratory, Tianjin University) [13] with this autocorrelator. The output average power of the laser is 500 mW, central

wavelength is 1060 nm, and pulse repeat frequency is 25 MHz. The intensity autocorrelation and the interferometric autocorrelation traces were shown in Fig. 13(a) and 13(b), respectively.

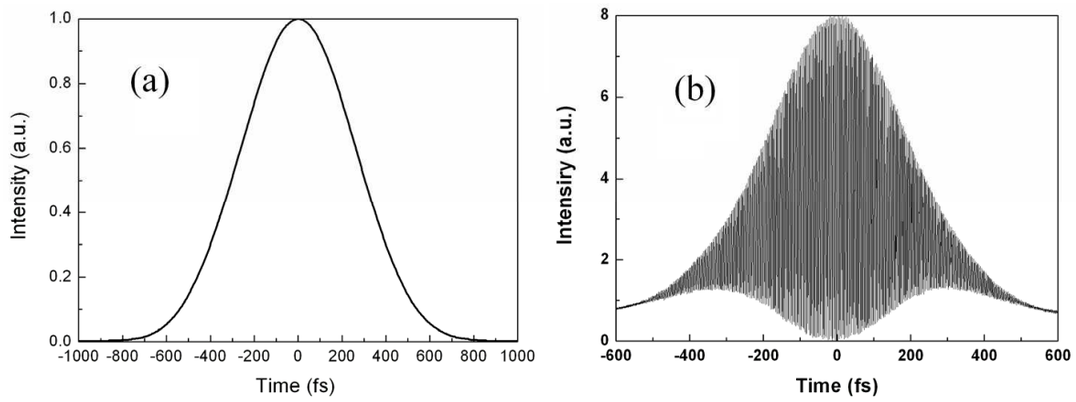

Fig. 13. Measured autocorrelations of photonic crystal fiber laser pulses. (a) Interferometric autocorrelation, (b) intensity autocorrelation.

Figure 13(a) gives a desirable intensity autocorrelation, which can clearly show the pulse width. The intensity autocorrelation applied a fast scanning of the translation stage; it is therefore much timesaving and suitable for fast measurement. The interferometric autocorrelation was shown in Fig. 13(b). The interferometric trace can be clearly discerned even the scanning length has extended to 1200 fs. From Fig. 13(b), we can see the dispersion compensation is acceptable except for a slight quadratic chirp. The interferometric autocorrelation trace in Fig. 13(b) gives phase information of the optical pulses, which is useful for the developing and optimizing of the laser.

This autocorrelator is based on a translation stage; therefore, the measurement range is related to the translation range of the stage. The stage we chosen has a translation range of 50 mm; therefore, the measurement range of the autocorrelator is 110 ps. By use of a two-photon detector and a lock-in amplifier, this autocorrelation has a higher sensitivity than THG one. The pulses with a 10 mW average power can be well measured.

4. Conclusions

The characterization technique of ultrashort optical pulses is introduced and demonstrated in this chapter. For accurate characterization of femtosecond optical pulses, we introduced a wavelet-transform technique for spectral phase retrieval. The wavelet-transform technique needs no filter; therefore, automatic and accurate phase retrieval and pulse reconstruction is realized because of no manual operation of selection and adjustment filter. With this technique, the ratio of autocorrelation width to pulse width can be determined, which is helpful in improving the precision of pulses width measurement with autocorrelation technique. We have demonstrated a multifunctional autocorrelator, based on a precise translation stage and a lock-in amplifier, for pulse width measurement of ultrashort optical pulses. With the autocorrelator, both interferometric autocorrelation and intensity autocorrelation can be obtained. Chirp can be clearly discerned form interferometric autocorrelation, and pulse width can be fast obtained from intensity autocorrelation. The

measurement result can self-calibrate with the two correlation traces. The autocorrelator is suitable for the measurement of ultrashort optical pulses from sub-10 fs to several hundred picoseconds, and it is useful in generation and characterization of both solid ultrashort pulse lasers and fiber ultrashort pulse lasers.

5. Acknowledgment

This work was supported in part by the National Science and Technology Supporting Program of China (grant 2006BAF06B05), Basic Research Foundation of National Institute of Metrology, China (grant AKY0748, AKY0904, and AKY1160).

6. References

[1] Ell R., Morgner U., Kärtner F. X., Fujimoto J. G., Ippen E. P., Scheuer V., Angelow G., Tschudi T., Lederer M. J., Boiko A., Luther-Davies B. (2001). Generation of 5-fs pulses and octave-spanning spectra directly from a Ti:sapphire laser, *Opt. Lett.*, Vol. 26, pp. 373-375

[2] Margolis H. S., Harper M. R., Lea S. N., (2006). Metrological applications of femtosecond optical pulse shaping, *NPL Report*, DEM-EM-010

[3] Hall J. L. and Ye J. (2001). A new era of frequency standards and optical frequency measurement, *Optics & Photonics News*, Vol. 12, pp. 44-50

[4] Yasui T., Yokoyama S., Inaba H., Minoshima K., Nagatsuma T., and Araki T. (2011). Terahertz frequency metrology based on frequency comb, *IEEE J. Sel. Top. Quant.*, Vol.17, pp. 191-201

[5] Williams D. F., Hale P. D., Clement T. S., and Morgan J. M. (2005). Calibrated 200-GHz waveform measurement, *IEEE T. Microw. Theory.*, Vol.53, pp. 1384-1389

[6] Diels J-C. M., Fontaine J. J., McMichael I. C., and Simoni F. (1985). Control and measurement of ultrashort pulse shapes (in amplitude and phase) with femtosecond accuracy, *Appl. Opt.*, Vol.24, pp. 1270-1282

[7] Kane D. J., Trebino R. (1993). Single-shot measurement of the intensity and phase of an arbitrary ultrashort pulse by using frequency-resolved optical gating, *Opt. Lett.*, Vol.18, pp. 823-825

[8] Iaconis C. and Walmsley I. A. (1999). Self-referencing spectral interferometry for measuring ultrashort optical pulses, *IEEE J. Quantum Electron.*, Vol.35, pp. 501-509

[9] Kärtner F. X. (2005) Chapter 10: Pulse Characterization Ultrafast Optics (Spring Term 2005), pp. 333-370

[10] Deng Y., Wu Z., Cao S., Chai L., Wang C. and Zhang Z. (2006). Spectral phase extraction from spectral interferogram for structured spectrum of femtosecond optical pulses, *Opt. Commun.* Vol.268 pp. 1-6

[11] Deng Y., Wu Z., Chai L., Wang C., Yamane K., Morita R., Yamashita M. and Zhang Z. (2005). Wavelet-transform analysis of spectral shearing interferometry for phase reconstruction of femtosecond optical pulses, *Opt. Express* Vol.13, pp. 2120-2126

[12] Meshulach D., Barad Y., and Silberberg Y. (1997). Measurement of ultrashort optical pulses by third-harmonic generation, *J. Opt. Soc. Am. B*, Vol.14, pp. 2122-2125

[13] Song Y., Hu M., Wang C., Tian Z., Xing Q., Chai L. and Wang C. (2008). Environmentally Stable, High Pulse Energy Yb-Doped Large-Mode-Area Photonic Crystal Fiber Laser Operating in the Soliton-Like Regime, *IEEE Photon. Tech. Lett.*, Vol. 20, pp. 1088-1090

Modern Metrology Concerns

Edited by Dr. Luigi Cocco

ISBN 978-953-51-0584-8
Hard cover, 458 pages
Publisher InTech
Published online 16, May, 2012
Published in print edition May, 2012

"What are the recent developments in the field of Metrology?" International leading experts answer this question providing both state of the art presentation and a road map to the future of measurement science. The book is organized in six sections according to the areas of expertise, namely: Introduction; Length, Distance and Surface; Voltage, Current and Frequency; Optics; Time and Relativity; Biology and Medicine. Theoretical basis and applications are explained in accurate and comprehensive manner, providing a valuable reference to researchers and professionals.

How to reference

In order to correctly reference this scholarly work, feel free to copy and paste the following:

Yuqiang Deng, Qing Sun, Shiying Cao, Jing Yu, Ching-yue Wang and Zhigang Zhang (2012). Measurement of Ultrashort Optical Pulses, Modern Metrology Concerns, Dr. Luigi Cocco (Ed.), ISBN: 978-953-51-0584-8, InTech, Available from: http://www.intechopen.com/books/modern-metrology-concerns/measuremet-of-ultrashort-optical-pulses

INTECH
open science | open minds

InTech Europe
University Campus STeP Ri
Slavka Krautzeka 83/A
51000 Rijeka, Croatia
Phone: +385 (51) 770 447
Fax: +385 (51) 686 166
www.intechopen.com

InTech China
Unit 405, Office Block, Hotel Equatorial Shanghai
No.65, Yan An Road (West), Shanghai, 200040, China
中国上海市延安西路65号上海国际贵都大饭店办公楼405单元
Phone: +86-21-62489820
Fax: +86-21-62489821

IntechOpen